Preprints of the 21st IFAC World Congress (Virtual)
Berlin, Germany, July 12-17, 2020

Robust positive control of a nonlinear tumor growth model ⋆

Dániel András Drexler * **Levente Kovács** *

* *Physiological Controls Research Center, Research and Innovation Center of Óbuda University, Óbuda University, Hungary (e-mails: {drexler.daniel,levente.kovacs}@nik.uni-obuda.hu).*

Abstract: Control of physiological systems, like tumor growth dynamics, can contribute to modern medicine by designing optimized therapies or automating treatments. Typical challenges in physiological control are the positivity of the input and the interpatient variability of model parameters. We use positive dynamics extension to ensure the positivity of the input, and design a robust controller for a nominal model acquired after exact linearization and stabilizing feedback. During the controller design, we minimize the effect of the model perturbation in the worst-case sense and minimize the energy of the performance criteria. The results show enhanced performance compared to our similar robust control approach where only the performance was minimized in the worst-case sense with similar characteristics in the input signals.

Keywords: Control of physiological and clinical variables; Kinetic modeling and control of biological systems; Healthcare management, disease control, critical care

1. INTRODUCTION

Control of physiological systems is becoming an inherent part of modern medicine. Clinically proven applications of physiological control are control of BIS in anesthesia (Alamir et al. (2018); Queinnec et al. (2018); Ionescu (2018)) and control of blood glucose level in artificial pancreas (Gondhalekar et al. (2018); Shi et al. (2018); Colmegna et al. (2018); Khan et al. (2018)). Control of tumor growth is an intensively researched area of physiological control as well, aiming to automatize therapies and optimize treatment protocols (Ren et al. (2017); Cacace et al. (2018); Klamka et al. (2017)).

In most physiological control problems the control signal is the injection of a drug, which can not be negative, which yields that the control input is constrained to be nonnegative. We handle this input constraint by using a dynamical extension of the model that ensures the positivity of the input first proposed in Drexler et al. (2017d) and used for tumor growth control in Drexler et al. (2017c, 2018); Kovács and Eigner (2018). We use a second-order model of tumor growth created for bevacizumab treatment in Drexler et al. (2017a) discussed in Section 2 for the control problem and extend it with positive input dynamics to get a third-order, nonlinear model in Subsection 3.1. This model is linearized using exact linearization (Isidori (1995)) in Subsection 3.2 and stabilized using state-feedback to get a linearized system with finite H_∞ norm. The model used here for controller design is a simplified model capturing the core dynamics of tumor growth which can be utilized to design model-based controllers that require many symbolic calculations. The more realistic, but more complex model validated with experimental data can be found in Drexler et al. (2017b) describing the effect bevacizumab and in Drexler et al. (2019) describing the effect of Pegylated Liposomal Doxorubicin.

Interpatient variability is also a critical problem in physiological control problems, which can be modeled as parametric uncertainties in most of the cases. We designed an H_∞-norm based controller for the linearized model with positive dynamics extension in Drexler et al. (2018), but we have only minimized the H_∞-norm of the closed-loop system with performance outputs. In order to reach better performance and handle uncertainty, we minimize the effect of model perturbation using H_∞-norm minimization and minimize the energy of the performance outputs using H_2-norm minimization in Section 3.3. Thus, interpatient variability is considered as an H_∞ minimization problem used e.g. in Dal Col et al. (2018); Colmegna et al. (2014); Kovács et al. (2014); Femat et al. (2009). Since exact linearization is based on exact cancellation of nonlinear terms, application of the exact linearization on the model will not result in a linear model in the presence of parametric perturbations, but the linearized model can be used as a nominal model for robust control design, and parametric uncertainties can be considered during the design of the robust controller as done in Subsection 3.3.

The designed controller is tested in silico with parametric perturbations of $\pm 20\%$ and compared to the results of the H_∞ controller from Drexler et al. (2018) which also utilizes positive control in Section 4. The simulations show that the proposed H_2/H_∞ controller gives significantly better performance with similar control inputs.

⋆ This project has received funding from the European Research Council (ERC) under the European Union's Horizon 2020 research and innovation programme (grant agreement No 679681). The present work has also been supported by the Hungarian National Research, Development and Innovation Office (2018- 2.1.11-T ÉT-SI-2018-00007 and SNN 125739).

2. MINIMAL TUMOR GROWTH MODEL

We use a minimal model of tumor growth proposed in Drexler et al. (2017a) for bevacizumab therapy. The model captures tumor proliferation, inhibiting effect of the drug and linear pharmacokinetics of the drug. The dynamics is described by the equations

$$\dot{x}_1 = ax_1 - bx_1x_2 \tag{1}$$
$$\dot{x}_2 = -cx_2 + u \tag{2}$$
$$y = x_1, \tag{3}$$

where x_1 denotes the time function of tumor volume in mm^3, x_2 denotes the time function of drug level in mg/kg, y is the measured output in mm^3 and u is the rate of drug injection measured in mg/(kg·day). The model parameters are the tumor growth rate a in 1/day, the inhibition rate b in kg/(mg · day) and the clearance c of the inhibitor in 1/day.

The value of the clearance parameter of intravenous bevacizumab injection is set to $c = \ln 2/3.9$ 1/day from Wu et al. (2012) and considered to be known in the simulations. The parameters identified based on mice experiments in Drexler et al. (2017a) are $a = 0.27$ 1/day and $b = 0.0074$ kg/(mg · day) and considered to be uncertain in the simulations.

3. ROBUST POSITIVE CONTROL

3.1 Positive input dynamics

In order to ensure the positivity of the control input, we extend the system with the dynamics

$$\dot{u} = -uv \tag{4}$$

with $u(0) > 0$, which has the solution

$$u(t) = u(0) \exp\left(\int_0^t v(\tau) d\tau \right) \tag{5}$$

which is always positive if $u(0) > 0$ (Drexler et al. (2017c,d, 2018)). We design the controller for the extended system

$$\dot{x}_1 = ax_1 - bx_1x_2 \tag{6}$$
$$\dot{x}_2 = cx_2 + u \tag{7}$$
$$\dot{u} = -uv \tag{8}$$

with the fictive input v and implement the extra dynamics (4) inside the controller to calculate the real input of the system. The states of the extended system are $x = (x_1, x_2, u)^\top$, and the state-space description of the extended system is

$$\dot{x} = f(x) + g(x)v, \tag{9}$$

with the drift vector field f and control vector field g defined as

$$f = \begin{pmatrix} ax_1 - bx_1x_2 \\ -cx_2 + u \\ 0 \end{pmatrix} \quad g = \begin{pmatrix} 0 \\ 0 \\ -u \end{pmatrix}, \tag{10}$$

while the output scalar field of the extended system is $h = x_1$.

3.2 Exact linearization and stabilization of the extended system

Let $L_f h$ denote the Lie derivative of the vector field f along the scalar field h, expressed as

$$L_f h = h' f, \tag{11}$$

and define the repeated application of the Lie derivative as

$$L_f^i h = \left(L_f^{i-1} h \right)' f \tag{12}$$

with $L_f^0 h := h$. Also, let

$$L_g L_f^i h = \left(L_f^i h \right)' g. \tag{13}$$

The relative degree of the output of the system (Isidori (1995)) in a point x is the integer r such that

$$L_g L_f^i h(x) = 0, \quad i = 0, 1, \ldots, r-2 \tag{14}$$
$$L_g L_f^{r-1} h(x) \neq 0. \tag{15}$$

The system is said to have maximal relative degree in a point if $r = n$, where n is the order of the system. If the system has maximal relative degree, then the system can be linearized in the point x using the state feedback

$$v = \frac{w - L_f^n h(x)}{L_g L_f^{n-1} h(x)} \tag{16}$$

and results in the linear system

$$\dot{z}_1 = z_2, \, \dot{z}_2 = z_3, \, \ldots, \, \dot{z}_n = w \tag{17}$$

where the new states can be acquired from the original states using the coordinate transformation

$$\begin{pmatrix} z_1 \\ z_2 \\ \vdots \\ z_n \end{pmatrix} = \phi(x) \begin{pmatrix} h(x) \\ L_f h(x) \\ L_f^2 h(x) \\ \vdots \\ L_f^{n-1} h(x) \end{pmatrix}. \tag{18}$$

This system is a series of integrators, which can be stabilized using the state feedback $w = -Kz + b_n \tilde{u}$, which results in the linear system

$$\dot{z} = \underbrace{\begin{pmatrix} 0 & 1 & \ldots & 0 & 0 \\ \vdots & & \ddots & & \vdots \\ 0 & 0 & \ldots & 1 & 0 \\ -k_n & -k_{n-1} & \ldots & -k_2 & -k_1 \end{pmatrix}}_{A} z + \underbrace{\begin{pmatrix} 0 \\ \vdots \\ 0 \\ b_n \end{pmatrix}}_{B} \tilde{u}, \tag{19}$$

with $K = (k_n, k_{n-1}, \ldots, k_1)$. The characteristic polynomial of the system matrix A is

$$s^n + k_1 s^{n-1} + k_2 s^{n-2} + \ldots + k_n \tag{20}$$

and the static gain of the linearized system is b_n/k_n, thus the transfer function of the linearized system is

$$G_n(s) = \frac{b_n}{s^n + k_1 s^{n-1} + k_2 s^{n-2} + \ldots + k_{n-1} s + k_n}. \tag{21}$$

For the extended minimal model described in Subsection 3.1, the Lie derivatives used for the coordinate transformation and feedback linearization are

$$L_f h = x_1(a - bx_2) \tag{22}$$
$$L_g h = 0 \tag{23}$$
$$L_f^2 h = x_1(a - bx_2)^2 - bx_1(u - cx_2) \tag{24}$$
$$L_g L_f h = 0 \tag{25}$$
$$L_g L_f^2 h = bux_1 \tag{26}$$
$$L_f^3 h = x_1(a - bx_2)(a^2 - 2abx_2 + b^2x_2^2 + cbx_2 - ub) + bx_1(u - cx_2)(c - 2a + 2bx_2). \tag{27}$$

Since $L_g h = 0$ and $L_g L_f h = 0$, but $L_g L_f^2 h(x) \neq 0$ for $x_1 \neq 0$, the extended system output has maximal relative degree everywhere except $x_1 = 0$ mm^3, and the extended system can be linearized. The coordinate transformation is

$$z = \phi(x) = \begin{pmatrix} h(x) \\ L_f h(x) \\ L_f^2 h(x) \end{pmatrix}, \tag{28}$$

while the feedback law with stabilization is

$$v = \frac{-Kz + b_3\tilde{u} - L_f^3 h}{L_g L_f^2 h}. \tag{29}$$

The poles of the series of integrators acquired after feedback linearization are transformed to -0.5 rad/day with multiplicity of three using the feedback gain

$$K = (\, 0.125 \;\; 0.75 \;\; 1.5 \,) \tag{30}$$

and the gain $b_3 = k_3$. The resulting system is a linear system with H_∞ norm being 1 and transfer function

$$G_n(s) = \frac{0.125}{s^3 + 1.5s^2 + 0.75s + 0.125}. \tag{31}$$

3.3 H_2/H_∞-norm based controller design

We design a two degrees of freedom (2-DOF) controller with the control law

$$\tilde{u}(s) = K_r(s)r(s) - K_y(s)y(s), \tag{32}$$

where r is the Laplace transform of the reference signal for the closed-loop system and y is the Laplace transform of the measured output of the system. The Laplace transform of the output of the controller is $\tilde{u}$, which is the input for the linearized system (21).

The system interconnection structure contains the controller with transfer function (32), the extended plant and a model uncertainty block. The extended plant consists of the nominal plant G_n and the sensitivity functions related to model uncertainty, sensor noise and performance. The inputs of the extended plant are the control input $\tilde{u}$, the sensor noise n, the reference signal r, and the disturbance input d that is used to represent model uncertainties through the model uncertainty block. The model uncertainty is represented as an output multiplicative uncertainty, the frequency content of the uncertainty is defined by the transfer function W_Δ. The output e of the extended plant is the input of the model uncertainty block.

The extended plant has two performance outputs: z_p and z_u, the tracking error and the control input performance, respectively. The frequency content of the tracking error performance is given by the transfer function W_p, while the frequency content of the control input performance is given by W_u. The tracking error is given as the difference of the outputs of the ideal closed-loop transfer function T_{id} and the nominal plant G.

The closed-loop system is considered to be the system where the extended plant and the controller are treated as one system M resulting after lower fractional transformation. The inputs of the closed-loop system are the signals d, n and r, while the outputs are the signals e, z_p and z_u. In the design phase, the H_∞-norm of the transfer function of the closed-loop system from the inputs to the output e is minimized to increase the robustness of the closed-loop system against model uncertainties in the worst-case sense, while the H_2-norm of the transfer function of the closed-loop system from the inputs to the outputs z_e and z_u is minimized to reduce the energy of the performance signals.

The measured outputs of the extended plant are the reference signal r and the sum of the nominal plant output and the sensor noise n that is filtered with the transfer function W_n in order to set the frequency content of the sensor noise. The measured outputs are the inputs of the controller K, while the output of the controller is the control input $\tilde{u}$ of the extended plant.

Denote the input of the closed-loop system M as $w = (e, r, n)^\top$ and partition the outputs of M as

$$z_\infty = e,\; z_2 = \begin{pmatrix} z_p \\ z_u \end{pmatrix}, \tag{33}$$

then the closed-loop system can be written as

$$\begin{pmatrix} z_\infty \\ z_2 \end{pmatrix} = \begin{pmatrix} M_1 \\ M_2 \end{pmatrix} w. \tag{34}$$

During H_2/H_∞ synthesis, we are searching for the controller K that minimizes the performance function

$$w_1\|M_1\|_\infty^2 + w_2\|M_2\|_2^2, \tag{35}$$

while ensuring that

$$\|M_1\|_\infty < \gamma_{\infty,max} \tag{36}$$
$$\|M_2\|_2 < \gamma_{2,max}. \tag{37}$$

The transfer functions used at the H_2/H_∞ controller design are

$$T_{id} = \frac{1}{10s + 1} \tag{38}$$
$$W_p = \frac{1}{(s+1)^2} \tag{39}$$
$$W_u = 0.5 \tag{40}$$
$$W_n = \frac{s+1}{0.1s+1} \tag{41}$$
$$W_\Delta = \frac{0.05\,(s+1)^2}{(0.1s+1)^2}. \tag{42}$$

The nominal plant G_n is acquired after feedback linearization and internal loop-shaping as described in Subsection 3.2. The ideal transfer function T_{id} of the closed-loop system, specified in (38), is chosen to have a gain of 1 and time constant of 10 days. Based on the experiments, the time constant of tumor growth is $1/0.27 = 3.7$ days, which is a time constant of an unstable dynamics. This dynamics is stabilized by the controller, and the speed of

the closed-loop dynamics was chosen to be slower than the untreated tumor growth in order to decrease the stress on the biological system caused by the therapy.

The performance weighting function W_p, specified in (39), is chosen such that the path tracking performance is 10 times faster than the reference model given by T_{id}. The model uncertainty weighting function W_Δ, given in (42), was chosen to describe that model uncertainties are present at high frequencies where good tracking is not required. The weighting functions W_p and W_Δ are chosen such that they do not result in contradiction in the design phase; the good tracking performance is required in low frequencies in which the model is known, and model uncertainties are present in high frequencies where good tracking is not demanded.

The weighting function W_n, given in (41), is chosen such that the effect of sensor noise is considered on frequencies higher than the frequencies where good performance is required. The W_u performance weight function of the control input, given in (40), is specified as a constant to limit the energy of the control input on every frequency.

The design parameters during the synthesis were

$$\gamma_{\infty,max} = 1,\ \gamma_{2,max} = 1,\ w_1 = 1,\ w_2 = 1. \tag{43}$$

The maximal γ values were chosen to be 1 so that the interpretation of the weighting functions is the same as in the case of H_∞-norm based controller design (Zhou et al. (1996)). The weighting parameters w_1 and w_2 were chosen to have the same value, so the H_2 and H_∞ norm specifications are considered with the same weight in the cost function (35) that is minimized during the controller synthesis.

The controller design resulted in the γ values

$$\gamma_\infty = 0.0532,\ \gamma_2 = 0.1632, \tag{44}$$

thus the required specifications are met by the closed-loop system. Moreover, the resulted γ_∞ value shows that the closed-loop system can tolerate larger model uncertainties than those modeled by the output multiplicative uncertainty with weighting function given in (42).

4. RESULTS OF SIMULATION

The positive robust controller was tested in-silico using simulations that run on a 300 days interval, with the tumor growth rate (a) and inhibition rate (b) parameters being varied by $\pm 20\%$. The reference signal is given as an exponential function

$$x_{1,ref}(t) = x_1(0) \exp(-t/100) \tag{45}$$

with $x_1(0) = 10000$ mm^3 being the initial tumor volume used in the simulations. The initial drug level was $x_2(0) = 0$ mg/kg, while the initial injection rate was $u(0) = 0.1$ mg/kg/day in the case of H_∞ controller and $u(0) = 8$ mg/kg/day in the case of the H_2/H_∞ controller.

The tumor volumes, inhibitor levels and the injection rates resulting after in-silico simulations for the H_∞-norm based controller described in Drexler et al. (2018) and the H_2/H_∞ controller described here are shown in Figs. 1, 2 and 3, respectively. The in-silico simulations show that the treatments based on the robust controllers are composed of two phases. First, there is a transient phase that lasts for about 50 days, and then the control input reaches its steady-state and the tumor volume decreases exponentially. The steady-states are similar for the two controllers, but the initial transient phase is different, especially if we consider the tumor volume evolution.

The most significant difference in the performance of the two controllers is that there was a large increase in the tumor volume in the initial transient in the case of the H_∞ controller, for the worst-case model perturbation (i.e., when the tumor growth rate increased and the effect of the drug decreased, the corresponding results indicated by the red curves in Fig. 1) the tumor volume increased by more than 200 %, however, in the case of the H_2/H_∞ controller this increase is less than 20 %. Moreover, while the H_∞ controller could only decrease the tumor volume after an initial transient where the tumor volume increased, in the case of the H_2/H_∞ controller the tumor volume only increased initially for the worst-case scenario. Figure 1 thus shows that the H_2/H_∞ controller gives much better performance, since the tumor volumes are significantly smaller, however, Figs 2 and 3 show that the required control inputs are similar, i.e., there was no need to apply larger doses to reach better performance. This result is fundamental for therapy optimization in practice and is the main motivation of the application of control theory to physiological control problems.

The difference between the controller design phases is that in the case of the H_∞ controller, only the performance was optimized using H_∞-norm, but without the model uncertainty, while in the case of the H_2/H_∞ controller, the performance was minimized in the H_2-norm and also model uncertainties were considered and the effect of uncertainty was minimized in the H_∞-norm. The main difference in the simulation scenario is the initial value of the injection rate: for the H_∞ controller, the initial injection rate was close to zero, thus the integrator in (4) needed time to increase the drug level in the patient that could partially explain that the tumor volume increased in the initial period.

5. CONCLUSIONS AND FUTURE WORKS

Most physiological control problems make the designer face two problems: positivity of the input and interpatient variability. Positivity of the input is guaranteed with the positive dynamics extension discussed in Subsection 3.1, which results in an extended system and introduces a nonlinear dynamics in the plant model used for controller design, while in the realization process the same nonlinear dynamics has to be implemented in the controller.

The interpatient variability, treated as model uncertainty is handled using methods from robust control, developed for linear systems. In order to use these linear control techniques on the nonlinear system, exact linearization is carried out followed by internal stabilization. Although exact linearization relies on exact cancellation of the nonlinear terms, in silico results show that the resulting control architecture can cope with model uncertainties and can generate positive control inputs.

In silico results showed that the appropriate initial value for the input can greatly affect the performance of the

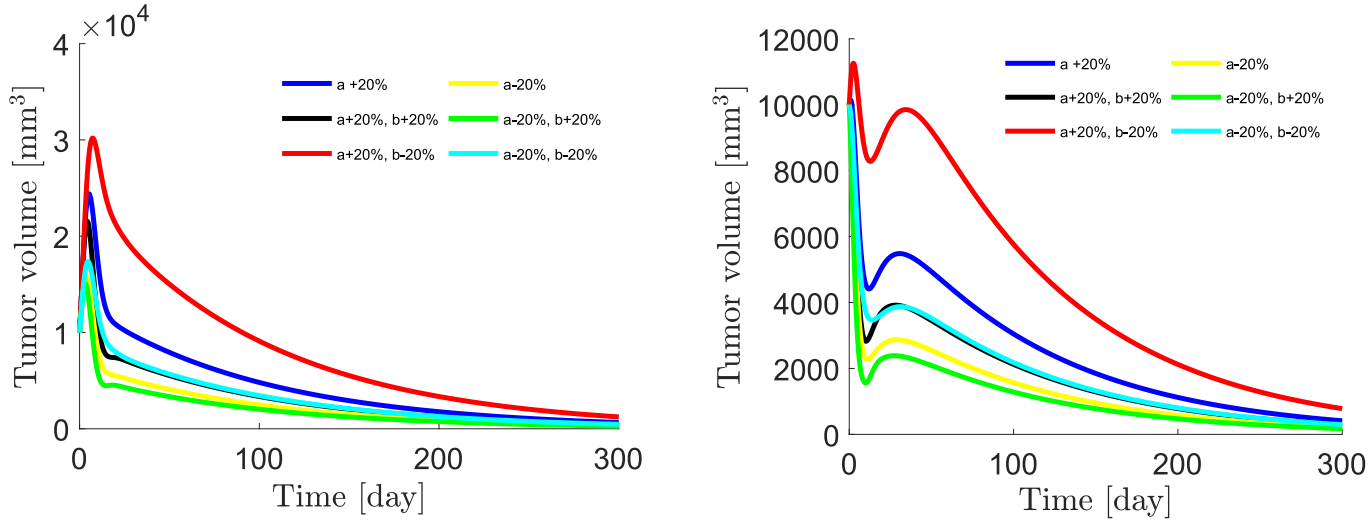

Fig. 1. The tumor volume during the 300 days therapy in the case of the H_∞ controller Drexler et al. (2018) (left) and the H_2/H_∞ controller (right)

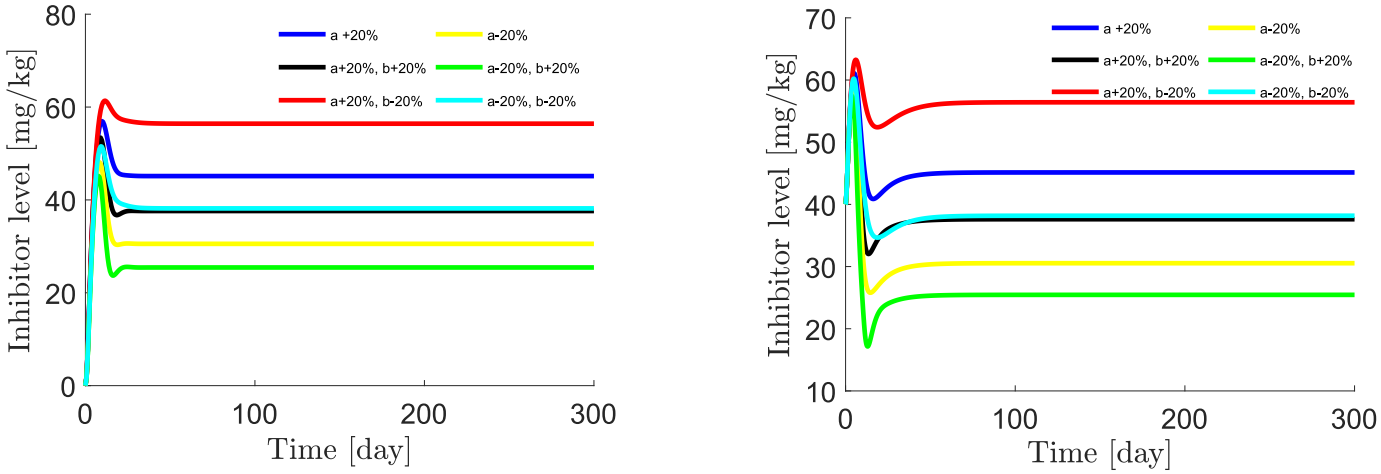

Fig. 2. The drug level during the 300 days therapy in the case of the H_∞ controller Drexler et al. (2018) (left) and the H_2/H_∞ controller (right)

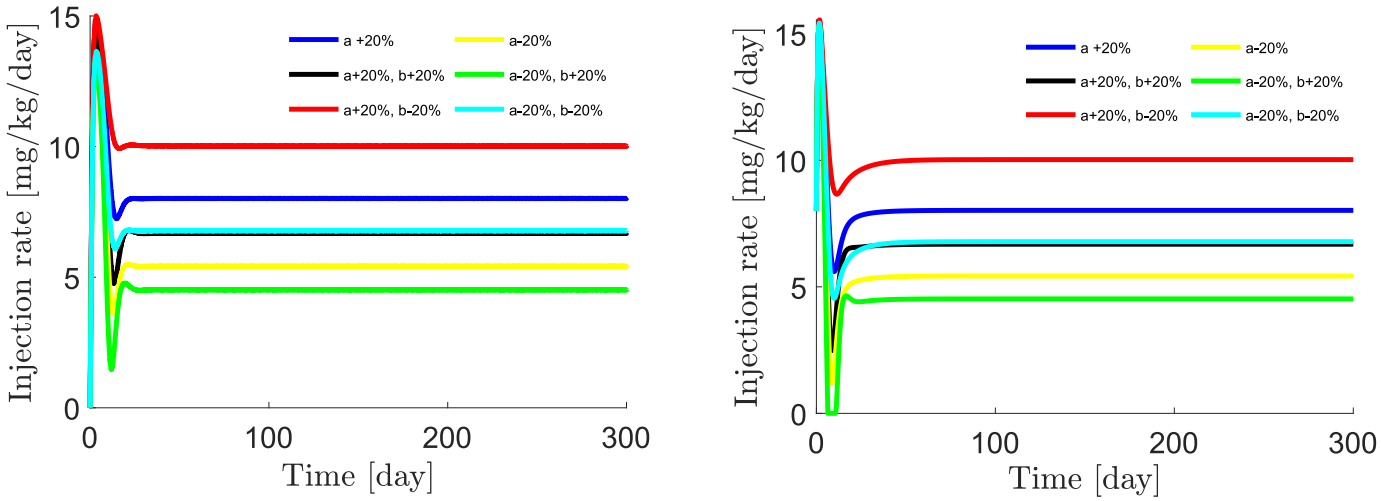

Fig. 3. The injection rate during the 300 days therapy in the case of the H_∞ controller Drexler et al. (2018) (left) and the H_2/H_∞ controller (right)

controller; by using larger initial injection dose, and changing the design scheme for the robust controller, the tumor volume evolution became more desirable which results in a great increase in the quality of life of a patient in practice. Moreover, this did not require larger doses or injections, the absolute values are similar, only the dynamical characteristics changed. This proves that the therapies can be optimized without the need for a significant increase in the applied doses.

REFERENCES

Alamir, M., Fiacchini, M., Queinnec, I., Tarbouriech, S., and Mazerolles, M. (2018). Feedback law with probabilistic certification for propofol-based control of bis during anesthesia. *International Journal of Robust and Nonlinear Control*, 28(18), 6254–6266. doi: 10.1002/rnc.4374.

Cacace, F., Cusimano, V., Germani, A., Palumbo, P., and Papa, F. (2018). Closed-loop control of tumor growth by means of anti-angiogenic administration. *Mathematical Biosciences & Engineering*, 15(4), 827–839. doi:10.3934/mbe.2018037. URL `https://doi.org/10.3934/mbe.2018037`.

Colmegna, P., Sánchez Peña, R.S., Gondhalekar, R., Dassau, E., and Doyle III, F.J. (2014). Reducing risks in type 1 diabetes using H_∞control. *IEEE Transactions on Biomedical Engineering*, 61(12), 2939–2947. doi: 10.1109/TBME.2014.2336772.

Colmegna, P., Garelli, F., Battista, H.D., and Sánchez-Peña, R. (2018). Automatic regulatory control in type 1 diabetes without carbohydrate counting. *Control Engineering Practice*, 74, 22 – 32. doi: https://doi.org/10.1016/j.conengprac.2018.02.003.

Dal Col, L., Queinnec, I., Tarbouriech, S., and Zaccarian, L. (2018). Regional H_∞ synchronization of identical linear multi-agent systems under input saturation. *IEEE Transactions on Control of Network Systems*, 1–11. doi: 10.1109/TCNS.2018.2877742.

Drexler, D.A., Sápi, J., and Kovács, L. (2018). H_∞ control of nonlinear systems with positive input with application to antiangiogenic therapy. In *Proceedings of the 9th IFAC Symposium on Robust Control Design ROCOND 2018*, 146 – 151. doi: https://doi.org/10.1016/j.ifacol.2018.11.096.

Drexler, D.A., Sápi, J., and Kovács, L. (2017a). A minimal model of tumor growth with angiogenic inhibition using bevacizumab. In *Proceedings of the 2017 IEEE 15th International Symposium on Applied Machine Intelligence and Informatics*, 185–190.

Drexler, D.A., Ferenci, T., Lovrics, A., and Kovács, L. (2019). Modeling of tumor growth incorporating the effect of pegylated liposomal doxorubicin. In *Proceedings of the IEEE 23rd International Conference on Intelligent Engineering Systems*, 369–374.

Drexler, D.A., Sápi, J., and Kovács, L. (2017b). Modeling of tumor growth incorporating the effects of necrosis and the effect of bevacizumab. *Complexity*, 1–11. doi: 10.1155/2017/5985031.

Drexler, D.A., Sápi, J., and Kovács, L. (2017c). Positive control of a minimal model of tumor growth with bevacizumab treatment. In *Proceedings of the 12th IEEE Conference on Industrial Electronics and Applications*, 2081–2084.

Drexler, D.A., Sápi, J., and Kovács, L. (2017d). Positive nonlinear control of tumor growth using angiogenic inhibition. *IFAC-PapersOnLine*, 50(1), 15068 – 15073. doi:https://doi.org/10.1016/j.ifacol.2017.08.2522. 20th IFAC World Congress.

Femat, R., Ruiz-Velazquez, E., and Quiroz, G. (2009). Weighting restriction for intravenous insulin delivery on t1dm patient via H_∞ control. *IEEE Transactions on Automation Science and Engineering*, 6(2), 239–247. doi:10.1109/TASE.2008.2009089.

Gondhalekar, R., Dassau, E., and Doyle, F.J. (2018). Velocity-weighting & velocity-penalty mpc of an artificial pancreas: Improved safety & performance. *Automatica*, 91, 105 – 117. doi: https://doi.org/10.1016/j.automatica.2018.01.025.

Ionescu, C.M. (2018). A computationally efficient hill curve adaptation strategy during continuous monitoring of dose-effect relation in anaesthesia. *Nonlinear Dynamics*, 92(3), 843–852.

Isidori, A. (1995). *Nonlinear Control Systems*. Springer-Verlag London.

Khan, H., Tar, J.K., Rudas, I., Kovács, L., and Eigner, G. (2018). Receding horizon control of type 1 diabetes mellitus by using nonlinear programming. *Complexity*, 11. doi:10.1155/2018/4670159. URL `https://doi.org/10.1155/2018/4670159`.

Klamka, J., Maurer, H., and Swierniak, A. (2017). Local controllability and optimal control for a model of combined anticancer therapy with control delays. *Mathematical Biosciences and Engineering*, 14(1), 195–216. doi:10.3934/mbe.2017013.

Kovács, L. and Eigner, G. (2018). Tensor product model transformation based parallel distributed control of tumor growth. *Acta Polytechnica Hungarica*, 15(3), 101–123.

Kovács, L., Szeles, A., Sápi, J., Drexler, D.A., Rudas, I., Harmati, I., and Sápi, Z. (2014). Model-based angiogenic inhibition of tumor growth using modern robust control method. *Computer Methods and Programs in Biomedicine*, 114, e98–e110.

Queinnec, I., Tarbouriech, S., and Mazerolles, M. (2018). Reference tracking controller design for anesthesia. In *Proceedings of the 9th IFAC Symposium on Robust Control Design ROCOND 2018*, volume 51, 158 – 163. doi:https://doi.org/10.1016/j.ifacol.2018.11.098.

Ren, H.P., Yang, Y., Baptista, M.S., and Grebogi, C. (2017). Tumour chemotherapy strategy based on impulse control theory. *Philosophical Transactions Mathematical Physical & Engineering Sciences*, 375(2088). doi:10.1098/rsta.2016.0221.

Shi, D., Dassau, E., and Doyle III, F.J. (2018). Multivariate learning framework for long-term adaptation in the artificial pancreas. *Bioengineering & Translational Medicine*, 0(0). doi:10.1002/btm2.10119.

Wu, F., Tamhane, M., and Morris, M. (2012). Pharmacokinetics, lymph node uptake, and mechanistic pk model of near-infrared dye-labeled bevacizumab after iv and sc administration in mice. *The AAPS Journal*, 14(2). doi:10.1208/s12248-012-9342-9.

Zhou, K., Doyle, J.C., and Glover, K. (1996). *Robust and Optimal Control*. Prentice-Hall, Inc., Upper Saddle River, NJ, USA.